JOURNAL OF CATALYSIS 55, 348–360 (1978)

Morphology and Sintering of Pt Crystallites on Amorphous SiO_2 [1]

M. CHEN AND L. D. SCHMIDT

Department of Chemical Engineering and Materials Science, University of Minnesota, Minneapolis, Minnesota 55455

Received March 17, 1978; revised July 20, 1978

Effects of O_2, N_2, H_2O, and Cl_2 atmospheres on sintering rates and morphologies of Pt on amorphous SiO_2 were studied by observation with transmission electron microscopy following heat treatment in flowing gases at 1 atm. An initial Pt film 10 to 20 Å thick produced crystallites 10 to 200 Å in diameter when heated to 400 to 700°C. The average crystallite size was larger by a factor of up to 2 in air than in N_2, and H_2O in these gases significantly inhibited particle growth. No crystallite migration was observed in any gases at any temperature. Atomic diffusion is therefore the exclusive sintering mechanism even though the size distribution exhibited a "tail" on the large diameter side which had been predicted by the particle coalescence model. Oxygen enhancement could occur through vapor transport as PtO_2 or through surface diffusion, although it is suggested that the latter is more plausible. Tilt experiments showed that all particles were three dimensional. Bright- and dark-field microscopy revealed that at least 20% of the particles heated to 600°C exhibited twinning, and multiple twins were observed in at least 2% of the particles. Good correspondence is observed between these results and behavior of supported catalysts.

INTRODUCTION

The loss of surface area due to crystallite growth is a major problem in design and use of supported metal catalysts. Because the crystallite size of interest is less than 100 Å, these processes are difficult to characterize, and the only direct studies have been by transmission electron microscopy (TEM). Crystallites have been observed on sectioned samples of porous supports such as carbon (*1*, *2*), alumina (*3–7*), and silica (*7–9*) using bright- and dark-field microscopy, but more definitive studies of these processes have been obtained using prototype supports consisting of thin planar substrates of materials such as Al_2O_3 (*10*, *11*). Sintering is strongly influenced by the presence of gases, and this has been examined either by transfer of the specimen into the microscope following heat treatment in gases (*10*) or by *in situ* observation in a controlled-atmosphere hot stage inside the microscope (*11*).

Two mechanisms of sintering have been identified: atom diffusion (*12–19*) and crystallite migration (*20–23*). Both predict that the surface area S should vary with time as

$$(S_0/S)^n = 1 + kt, \qquad (1)$$

where S_0 is the initial area, k is a constant, and n is an integer which depends upon the model. Experimental values of n have been in the range of 1 to 14, although the atomic diffusion model predicted n values between 2 and 4 depending on the rate-limiting step assumed (*12*, *16*, *17*). Recently Wynblatt

[1] Partially supported by NSF under Grant ENG75-01918.

0021-9517/78/0553-0348$02.00/0

and Gjostein (*18, 19*) calculated higher and time-dependent n values assuming a growth limited by nucleation of new metal layers on crystallite facets. Crystallite migration and coalescence were considered by Ruckenstein and Pulvermacher (*20–23*) who, assuming Brownian motion of particles with coalescence upon collision, obtained n values of 1 to 7 with various assumptions. Evidence for both growth mechanisms has been inferred from n values obtained using metal surface-area measurement, X-ray line broadening, electron microscopy, etc. Sintering of Pt on graphitized carbon black in H_2 and N_2 was studied by Bett *et al.* (*2*) who found results that could be fit with $n = 4$ which they interpreted as indicating crystallite migration. The mobility of Pt, Ag, Au, etc. on graphite and amorphous carbon has also been reported (*24–30*) by direct observation of the motion of metal crystallites inside the electron microscope under various conditions. Pt supported on Al_2O_3 has been studied extensively for both porous (*31–35*) and thin planar supports (*10, 11, 36*). Results show that growth rates are considerably higher in O_2 than in inert atmospheres with typical n values of 1 in air (*31*) and 5 to 7 in H_2 (*32, 33*) for Pt on porous alumina. Baker *et al.* (*11*) and Wynblatt and Gjostein (*10*) examined sintering in some detail by depositing Pt on a thin γ-Al_2O_3 support. Baker *et al.* (*11*) used controlled-atmosphere electron microscopy and found that Pt crystallites larger than 25 Å were immobile on the surface of Al_2O_3 up to 920°C in 2 Torr of O_2 and N_2. Wynblatt and Gjostein (*10, 19*) found that their results in O_2 could be fit with the atomic diffusion model assuming nucleation-controlled growth with PtO_2 the transport species.

In this paper we examine sintering rates and growth mechanisms of Pt on amorphous SiO_2. This system has been studied mainly in porous supports (*9, 37–39*). Dorling *et al.* (*37, 38*) observed the influence of various methods of catalyst preparation and sintering conditions on crystallite size. Platinum on silica catalysts prepared by ion exchange were found to have better initial dispersion and higher resistance to sintering than those prepared by impregnation (*9, 38, 39*). However, from past studies, the relative importance of atomic diffusion versus crystallite migration and effects of gases in growth processes cannot be assessed.

EXPERIMENTAL

In most experiments Pt was vacuum deposited on amorphous SiO_2 which had been prepared by oxidizing a thin disk of Si. Specimens were heated in flowing gases at 1 atm in a furnace for specified time and temperature and were then transferred to the electron microscope for observation. A single specimen was typically heated and examined repeatedly to observe effects of time and temperature on a particular region.

Thin-film sections of silicon were prepared by cutting a specimen of (111)-oriented single-crystal Si (resistivity 1000 to 3000 Ω-cm) into a disk with a thickness of ~0.5 mm and a diameter of 3 mm, then chemical etching in a HNO_3 and HF solution jet to a thickness of about 2000 Å. The disk was then ion micromilled in an Ar ion discharge until a pinhole at the center of the disk was observed (*40*). Samples with regions near the pinhole sufficiently thin for microscopy ($\lesssim$500 Å) were then thermally oxidized in air in a quartz furnace at 1100°C for 1.5 hr. This procedure would produce an amorphous layer of SiO_2 about 1000 Å thick (*41*). Electron diffraction in the microscope confirmed that no spot pattern characteristic of silicon remained and that only the diffuse ring of amorphous SiO_2 was present. A thin film of Pt was then deposited on one side of the support in a vacuum evaporator. Pt thicknesses were estimated from the size of Pt particles assuming a hemispherical shape after heating the sample above 550°C. When several

specimens of identical Pt loading were desired, Pt was deposited simultaneously onto several SiO_2 supports.

Samples were heated in a quartz tube 3 cm in diameter and 90 cm long through which gases were made to flow at a total rate of ~0.5 cm^3/sec. Cylinder gases (purity at least 99.9%) were used without further purification. Temperatures were measured with a thermocouple inside the quartz tube. Specimens were examined in a RCA-4U transmission electron microscope with resolution of about 15 Å for measuring the size distribution and average Pt particle size. A JEM-100C scanning transmission microscope (STEM) with a resolution of 3.4 Å was also used to observe the morphology and internal structure of crystallites.

Samples were not exposed to aqueous environments after oxidation of the Si, and the SiO_2 substrates were self-supporting to eliminate possible contamination from grids. However, exposure of specimens to laboratory air at various stages of preparation and treatment may of course produce contamination. We do not believe that this affected results significantly because experience in this laboratory suggests that such treatment does not produce gross contamination of Pt and because analyses of several specimens by scanning Auger microanalysis (SAM) and by X-ray fluorescence in the STEM system indicated negligible contamination. X-Ray fluorescence showed only Si and Pt peaks while SAM showed Si, Pt, O, and less than monolayer of C. No other impurities were detected within the sensitivity limits of the techniques.

Contamination and damage could also arise during electron microscopy. Carbon contamination was kept low by maintaining the pressure of the specimen chamber of the microscope in the 10^{-7}- to 10^{-8}-Torr range. Most experiments were duplicated with both low and high electron fluxes to show that no bombardment effects were evident. For results reported here the specimen irradiation was maintained at a level much below that where any electron bombardment effects were noted.

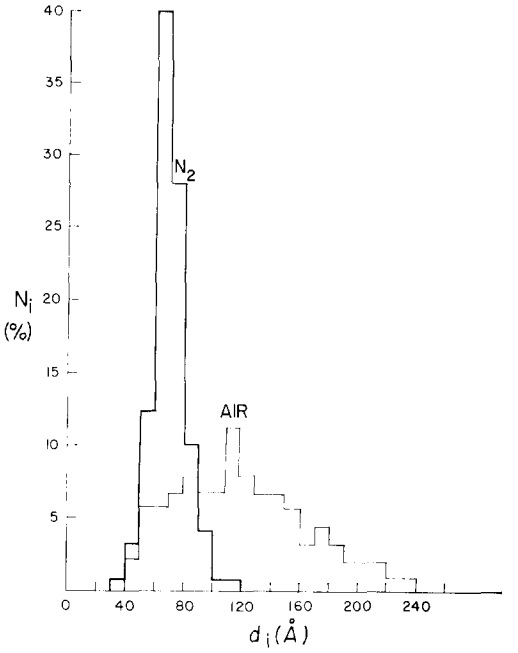

FIG. 1. Comparison of size distribution histograms for sintering in dry air and in dry N_2 at 700°C.

RESULTS

Gas and Temperature Dependences

A set of samples with an identical platinum film thickness of about 10 Å was heated in different gas environments for 1 h at various temperatures. Crystallite size distributions were obtained by counting the Pt particles on the same area of the substrate after each heat treatment. Approximately 300 particles were counted at 600°C, although the number depended on the stage of sintering. The histograms in Fig. 1 compare size distribution between sintering in air and in N_2. For treatment in N_2 the size distribution is narrow and nearly symmetric, while in air the distribution is broader and more asymmetric. Figure 2 shows smoothed size distributions at various temperatures for sintering in air.

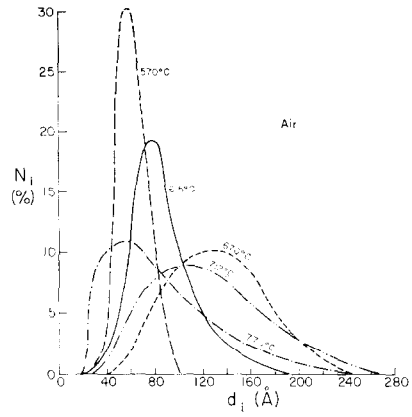

FIG. 2. Smoothed histograms of size distribution at various temperatures for sintering in dry air.

Figure 3 shows the average Pt crystallite diameter $\bar{d}$ versus temperature in the gases indicated. From Fig. 3 it is clear that the crystallite growth rate is higher for sintering in air than in N_2. Similar behavior has also been reported by others for Pt supported on Al_2O_3 (*10, 11*) [Figure 2 of Ref. (*11*) contains an error which indicates a higher rate in N_2 than in air]. The average crystallite size is observed to decrease upon heating in air above 730°C. This is probably due to the formation of volatile oxides and their escape at higher temperatures. To investigate water vapor effects, the gases were bubbled through distilled water which was maintained at 90°C. Figure 3 also shows that water vapor significantly inhibits the growth rate of the Pt crystallites in both N_2 and air.

Results of another set of experiments with higher Pt loading (initial film thickness ~15 Å) on SiO_2 are shown in Fig. 4. The effects of O_2 and water vapor on the growth rate are essentially identical to those just described. Similar experiments were repeated on many SiO_2 substrates with various Pt loadings. In no cases did results differ significantly from those shown in Figs. 1 to 4.

The morphology of Pt crystallites after sintering was also examined in the JEM-100C STEM. Figure 5 shows the difference in morphology following treatment of crystallites in wet air and wet N_2 at temperatures up to 830 and 1050°C, respectively. (The heating histories of these two samples correspond to curves a and c of Fig. 4.) Electron diffraction showed only rings of face-centered cubic (fcc) Pt and amorphous SiO_2. Most crystallites had roughly hexagonal shapes after heating in N_2 at a temperature of 1050°C. However, some of the Pt crystallites exhibited irregular shapes when sintered in air. They

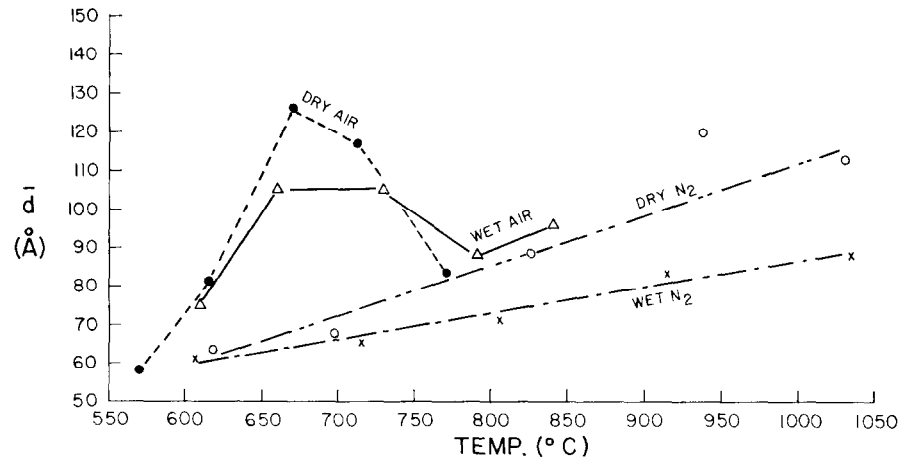

FIG. 3. Average Pt crystallite diameter $\bar{d}$ versus sintering temperature for gas environments indicated for an initial Pt film thickness of 10 Å. Histograms for dry air are shown in Fig. 2.

also showed more complicated contrast while only a few particles sintered in N_2 exhibit this contrast. Water vapor did not produce any apparent change in morphology or shape of the particle size distribution.

The heights of the particles were estimated by tilting the specimen inside the microscope by 45°. The ratios of measured particle diameter with 45° tilt, d_{45}, to the diameter without tilt, d_0, were then measured. Figure 6 shows the ratio d_{45}/d_0 versus particle diameter d_0. The measurements indicate that the particles were three dimensional and that the ratios were nearly independent of particle size and of gas atmosphere.

A series of experiments was also run with 10% Cl_2 in N_2 and in air. After heating to 650°C, no platinum particles remained on the substrate in either gas mixture. This is believed due to the formation of volatile platinum chlorides which escape from the substrate. Analysis of the sample which had been heated in Cl_2 and air mixture revealed only the Si peak. No Cl or Pt remained on this surface. (Oxygen is not detectable with this technique.) In the absence of O_2, Cl_2 reduced the SiO_2 substrate to $SiCl_4$ at 650°C.

Experiments were also performed with Pt deposited by argon ion sputtering and also from H_2PtCl_6 solution. Argon ion bombardment of a high-purity Pt target was used to deposit Pt onto the SiO_2 substrate inside the high-vacuum microscope stage with an argon pressure of $\sim 6 \times 10^{-6}$ Torr. (The vacuum before sputtering was $\sim 5 \times 10^{-8}$ Torr.) For Pt prepared from chloroplatinic acid, a drop of 0.12% H_2PtCl_6 solution was placed on the SiO_2 and then dried at 100°C. Platinum prepared by both of these techniques yielded crystallite sizes and morphologies indistinguishable from those prepared by vacuum evaporation in that heating in air produced larger sized particles than in N_2 for comparable temperatures.

Time Dependence

In this set of experiments, samples with the same initial Pt film thickness of about 15 Å were heated at a fixed temperature of 650°C for various times in air and in N_2.

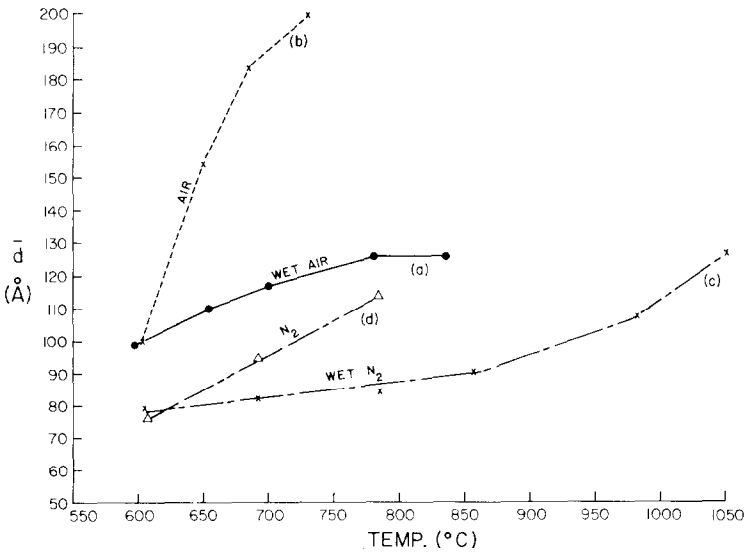

FIG. 4. Average Pt crystallite diameter $\bar{d}$ versus sintering temperature for gas environments indicated for an initial Pt film thickness of 15 Å.

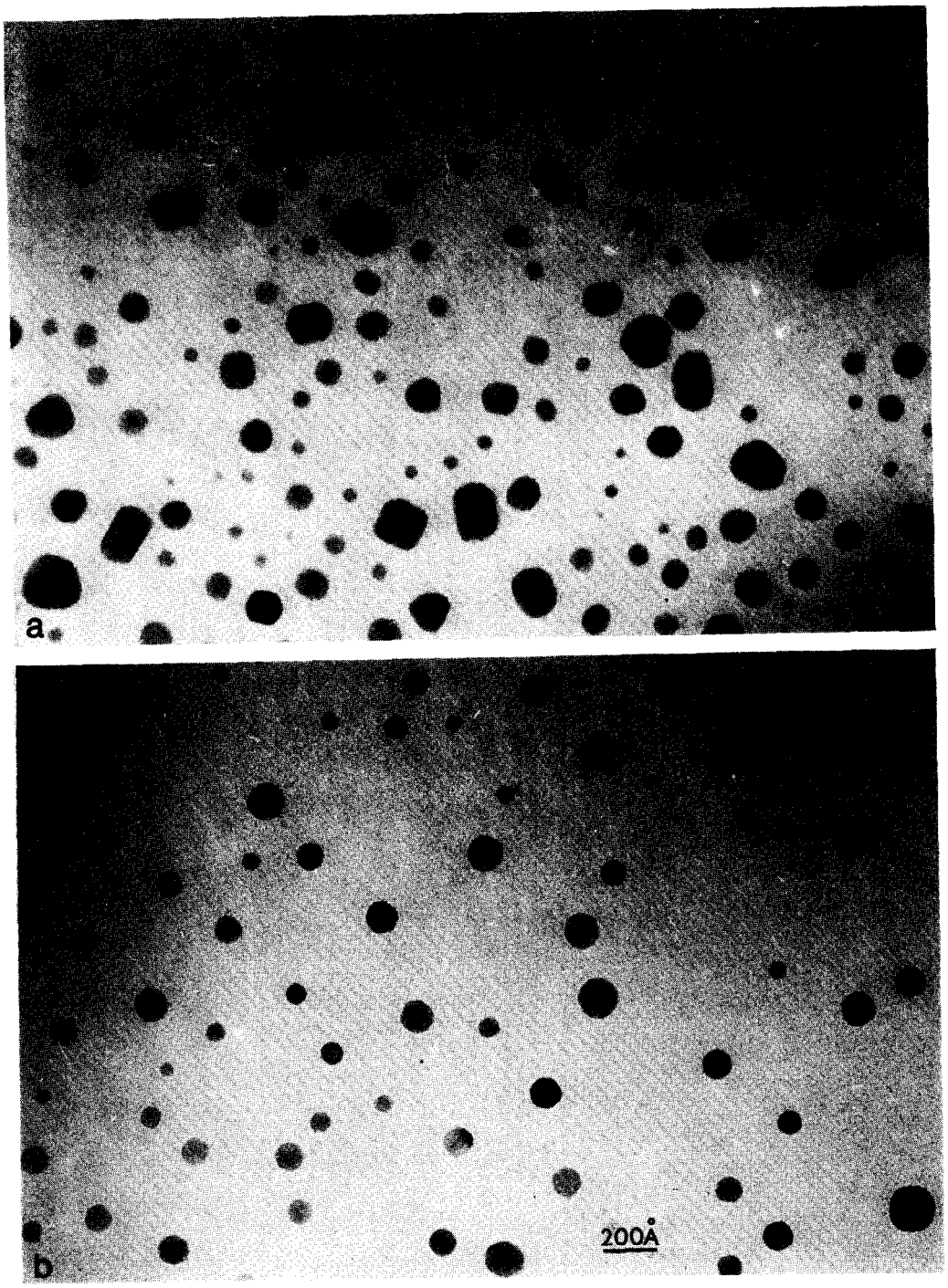

FIG. 5. Micrographs of Pt crystallites on SiO_2 after sintering (a) in wet air at 830°C and (b) in wet N_2 at 1050°C for an initial Pt film thickness of 15 Å. Particles are larger and exhibit more twins in air than in N_2.

Growth curves are shown in Fig. 7. Plots of log $\bar{d}$ versus log t gave $n = 6$ and 10 for heating in air and in N_2, respectively. The morphology after heating for 8 hr in air and in N_2 is also illustrated in Fig. 8. The Pt particles sintered in air after 8 hr at 650°C have essentially the same morphology as those obtained by heating in air under fixed-time, varying-temperature experiments. However, Pt particles sintered in N_2 at relatively low temperature (650°C) did not attain a hexagonal shape after an 8-hr treatment. About 20% of the Pt particles showed various kinds of contrast variations on the electron micrograph. These contrast variations arise from diffraction contrast,

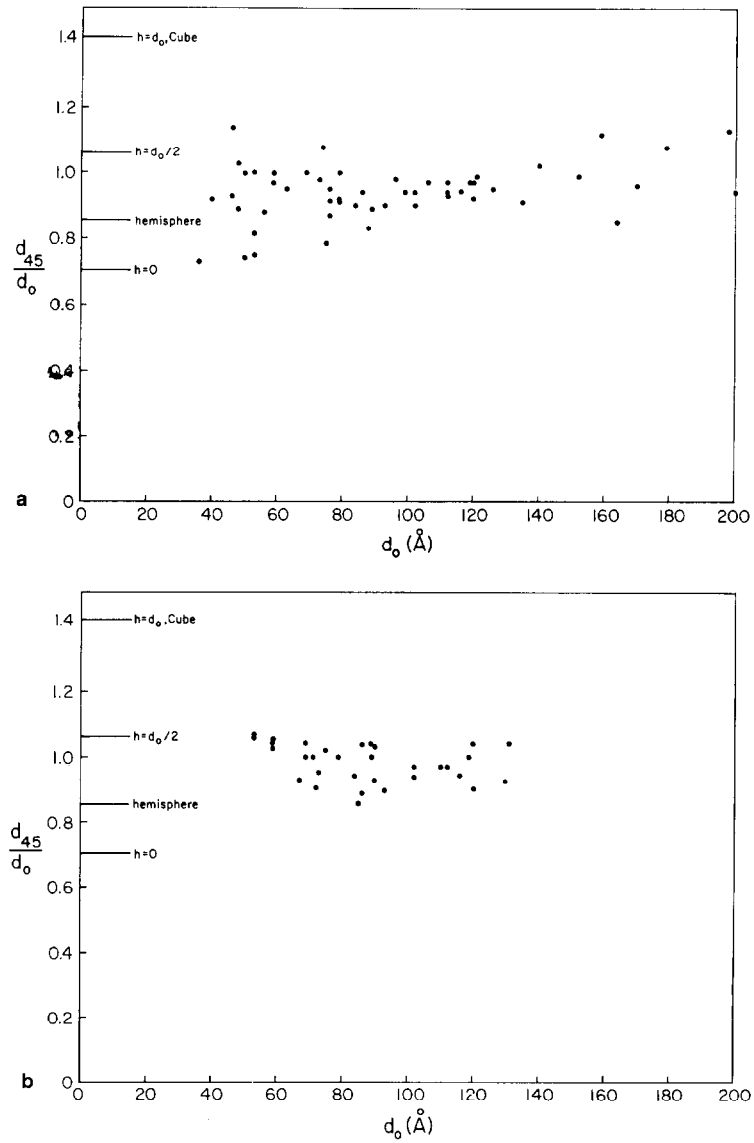

FIG. 6. Estimation of the height of Pt crystallites on SiO_2 after sintering (a) in wet air at 830°C and (b) in wet N_2 at 1050°C. Points shown are ratio of diameter at 45° to the electron-beam axis to the diameter at normal incidence. All particles appear to be three dimensional with a thickness approximately $\frac{1}{3}$ of the diameter.

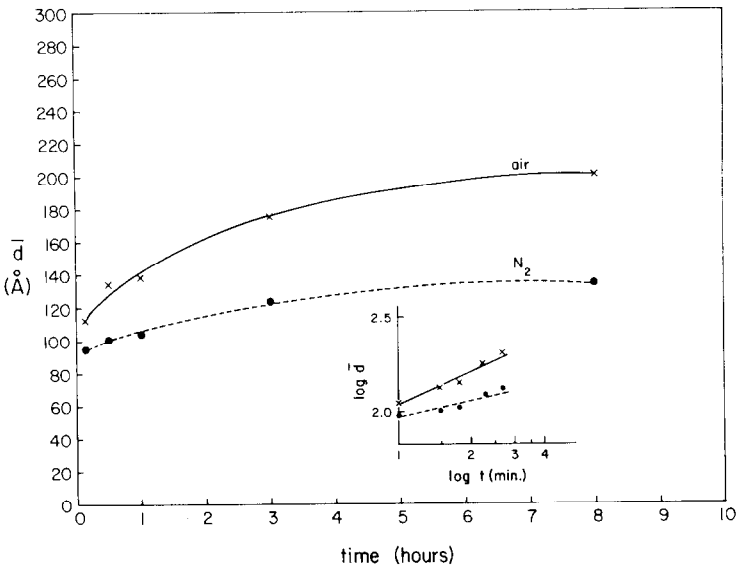

FIG. 7. Effect of sintering time on the growth of Pt crystallites at 650°C in air and in N_2. Inset shows a log–log plot which gives exponents n of 6 and 10, respectively.

and they indicate these crystallites are actually bicrystals, probably twins (*42*). An attempt was made to compare the fraction of bicrystals by heating samples in air and in N_2 at temperature 600°C for 1 hr. Again a broader particle size distribution was obtained by sintering in air than in N_2, but the morphology and contrast variation of Pt particles were similar, and the fraction of Pt particles with contrast variations was nearly the same (~20%) for treatment in these two gases. Particles with multiply twinned structure (*43–46*) were observed in about 2% of total particles, similar to results reported by Avery and Sanders (*47*).

Crystallite Motion

The possible motion of particles was examined in a number of experiments by observing the same area of the sample between various heat treatments. Figure 9 illustrates the growth processes of Pt crystallites sintered in air for a heating time at each temperature of 1 h. Since every crystallite remaining on SiO_2 maintained its position while some particles exhibited size variation, it is clear that the growth is completely by atom diffusion rather than particle migration. The minimum sized particle which could be shown to remain in its position was about 15 Å. The only instances of coalescence occurred when two or more nearby particles grew until they made contact. Under this situation the size of the resulting particle was sometimes smaller than the sum of the initial diameters as shown in Figs. 9b and c.

DISCUSSION

Mechanisms of Enhanced Growth and Evaporation

Oxygen produces an enhancement of the particle growth rate above 500°C and a decrease in size due to volatization above 700°C. Chlorine produces significant volatization below 600°C. Water in either air or N_2 significantly reduces the growth rate. Similar effects of O_2 on the growth of Pt have been noted on Al_2O_3 also (*10, 11*).

Metal loss almost certainly occurs through PtO_2 and $PtCl_4$, respectively, but growth could proceed through either vapor

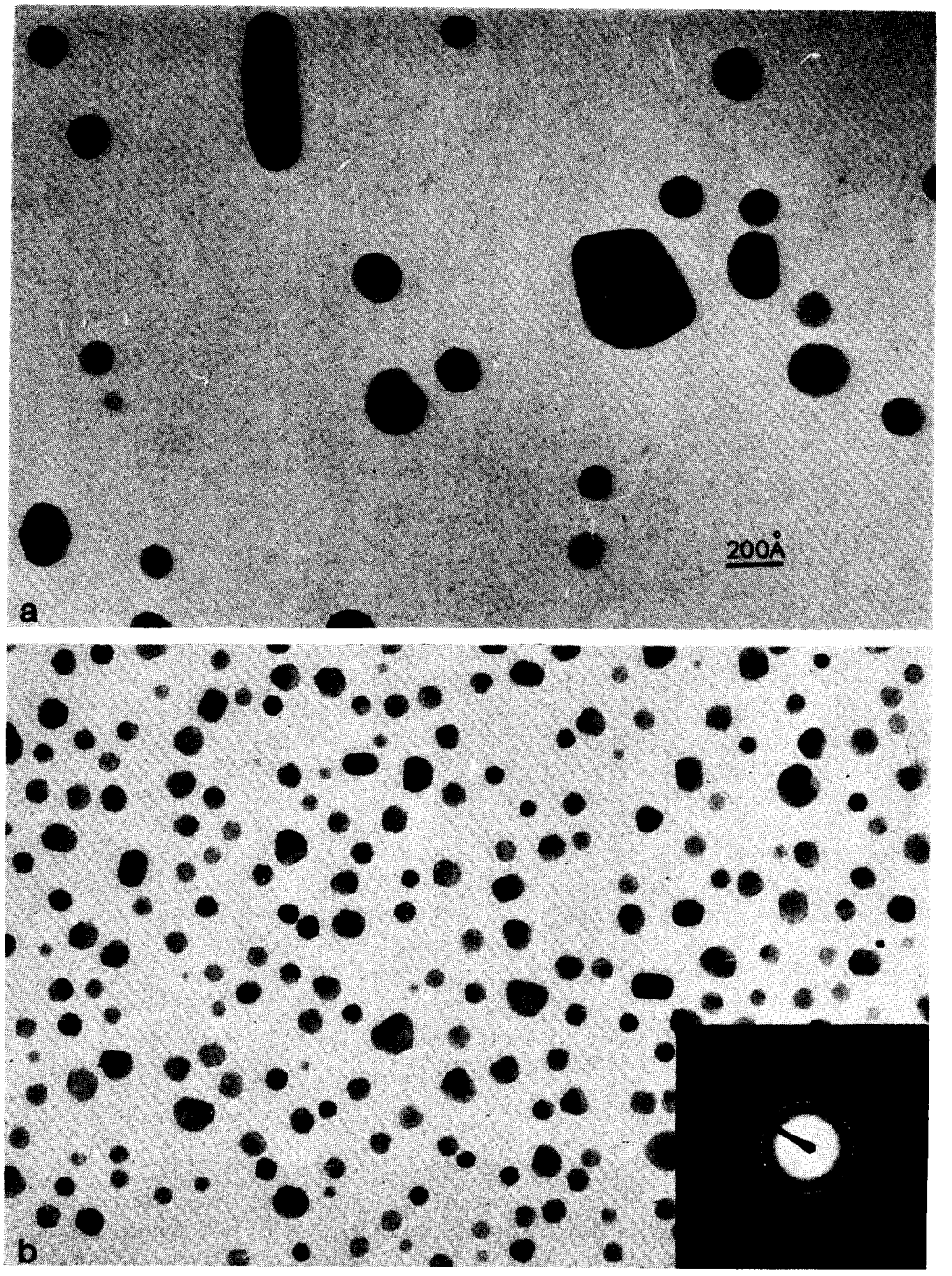

FIG. 8. The morphology of Pt crystallites on SiO_2 at 650°C after 8 h of sintering (a) in air and (b) in N_2. Diffraction pattern in inset in (b) shows only the fcc rings of Pt and the broad ring of amorphous SiO_2.

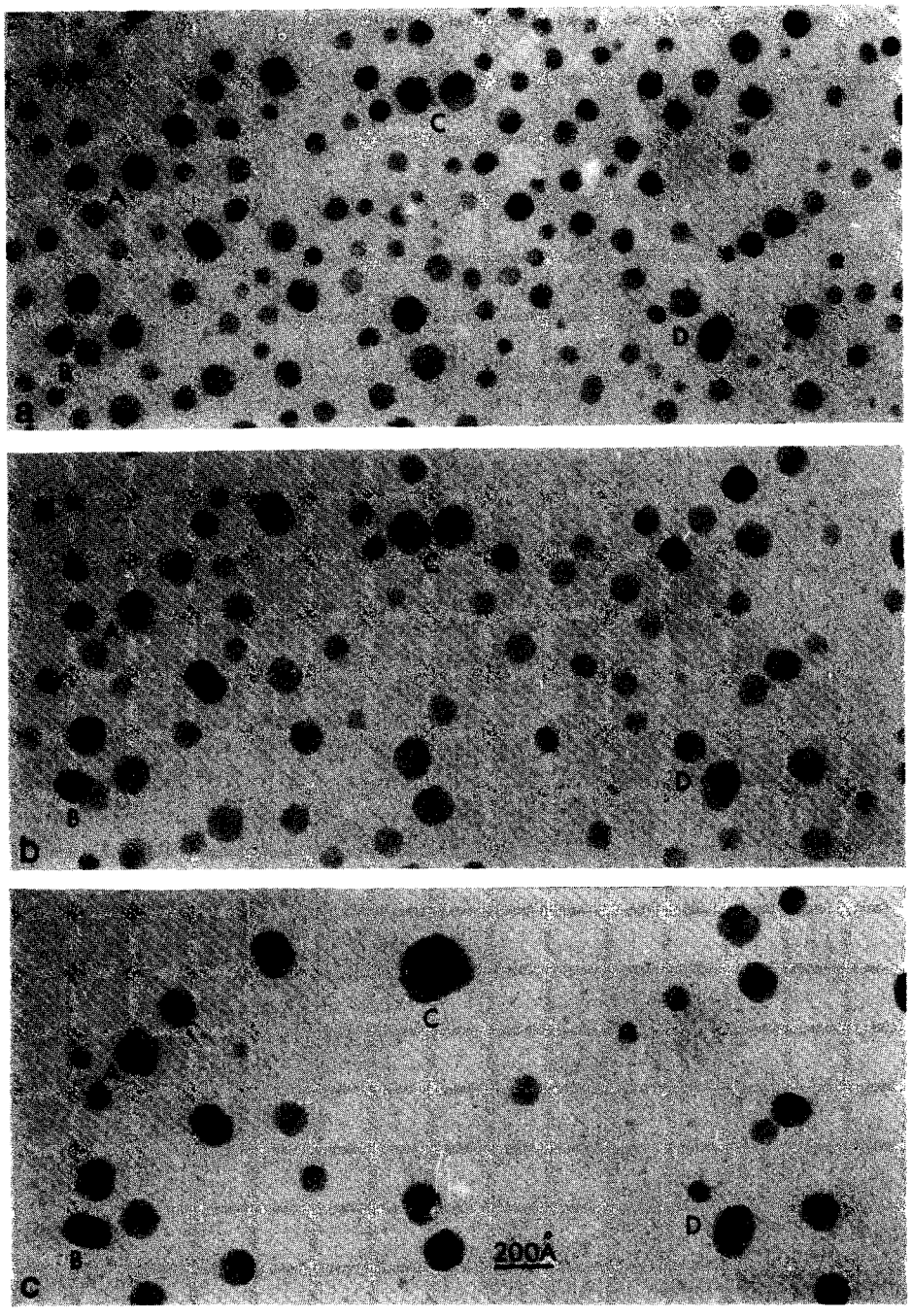

FIG. 9. The growth of Pt crystallites on SiO_2 in air at (a) 600°C, (b) 650°C, and (c) 685°C for 1 h at each temperature. The growth mechanisms are exclusively through atom diffusion rather than crystallite migration shown in regions A and D, although some regions such as B and C show that when two crystallites touch, they coalesce to give a size smaller than the sum of the initial diameters.

transport of PtO_2 or through surface diffusion. As discussed by Wynblatt (*16–18*), there are several possible rate-limiting steps in particle growth. The vapor pressure of Pt is only 10^{-11} Torr even at 1050°C, and therefore the growth mechanism in the absence of O_2 must be surface diffusion of Pt on the SiO_2 substrate. The inhibition by H_2O in either air or N_2 is probably caused by a reduced Pt surface diffusion coefficient on SiO_2, possibly associated with adsorbed H_2O and OH groups adsorbed on the SiO_2 surface.

In oxygen at 0.2 atm, the vapor pressure of PtO_2 is 2×10^{-9} Torr at 500°C and 4×10^{-7} Torr at 700°C. These represent maximum evaporation fluxes of 10^{-4} and 0.02 monolayer/s, respectively. Since the observed rates of disappearance of Pt are in the range of a few monolayers per hour, these values would be consistent with maximum fluxes. However, the question of volatile oxide transport is complicated by the existence of a stagnant boundary layer when the specimen is heated in flowing air. Flow in these experiments is laminar, and we estimate the boundary layer thickness to be between 0.1 and 1 mm. The rate of transport between particles and the rate of evaporation must be calculated by solving the diffusion equation in this layer for a particular geometry. A simple model assuming particles 100 Å in diameter from which evaporation is occurring onto particles 100 Å away and through a boundary layer yields a rate of deposition on adjacent particles between 10 and 100 times lower than the flux calculated from the vapor pressure of PtO_2. The evaporation rate is in turn lower by a factor of $\sim$1000 than the flux calculated from the vapor pressure of PtO_2.

These estimations lead to vapor transport rates significantly below the growth rates observed experimentally. However it is difficult to describe the boundary layer accurately, and the geometry, thermodynamics, and nucleation properties of small particles are not well characterized. Therefore it is not possible to entirely eliminate vapor transport as a growth mechanism.

It appears more likely, however, that oxygen enhances the sintering rate of Pt by increasing the mobility of Pt atoms over the surface. This mechanism also provides a rationale for the inhibition of sintering by H_2O. It is difficult to visualize how H_2O could alter the vapor transport processes of Pt significantly, but it could alter the surface diffusion coefficient of Pt on SiO_2.

Comparison with Pt Supported on Porous SiO_2 Catalysts

While the gas environments and temperatures in these experiments are close to those encountered in preparation and operation of metals on porous oxide supports, it should not be expected that an exact correspondence exists between these results on a planar SiO_2 substrate and processes on porous SiO_2. Both substrates are amorphous, although porous SiO_2 contains H_2O in the structure as well as on the surface, while planar substrate prepared by air oxidation of Si can probably only adsorb a limited amount of H_2O.

The sintering process within the pores of a porous catalyst involves a more tortuous transport path, and particle shrinkage and growth can occur with negligible evaporation from the porous matrix. The sintering behavior of Pt on SiO_2 (*9, 37–39*) has been less extensively studied than that of Pt on on Al_2O_3 (*10, 11, 31–36*). However, a fairly good agreement is noted between our results and those reported by Dorling *et al.* (*37, 38*). They reported that for Pt supported on silica, sintering in air had a detrimental effect on dispersion for catalysts prepared by both impregnation and adsorption methods. Furthermore, their Pt particle size versus sintering temperature curve shows the same behavior as ours in that the average size increases with temperatures

up to 700°C, and the size and amount of Pt decreases due to volatization of Pt oxide upon heating above 700°C. While processes on our substrate are certainly simpler than those on porous SiO_2 and the loadings of Pt are not directly comparable, the particle sizes versus temperature and gas environment agree reasonably well. Recently, Sashital *et al.* (*48*) used X-ray diffraction methods to study the Pt/silica system. Their results also showed that Pt particles are three dimensional and exhibit twin boundary defects for crystallite diameters of ~120 Å.

It is known that Pt sinters more readily on SiO_2 than on Al_2O_3 catalyst supports. The difference in growth rate of Pt particles on planar supports of amorphous SiO_2 and γ-Al_2O_3 could be obtained by comparing our results with those reported by Wynblatt and Gjostein (*10*) under similar experimental conditions. In air we obtained average particle diameters of 140 and 200 Å at 650°C after 1 and 8 hr, respectively, while they reported 85 and 120 Å at 700°C after the same time periods. In both systems, the average particle diameters increase by a factor of ~1.4 between 1 and 8 hr, while the sintering temperature is 50°C lower for Pt on SiO_2. Thus sintering appears to be enhanced on both planar and porous SiO_2 compared to Al_2O_3.

It is usually found that H_2O decreases the sintering rate of metals on oxide catalyst supports (*49*). However Dorling *et al.* (*38*) noted enhanced sintering only if the Pt/silica catalysts prepared by the impregnation method had not been thoroughly dried prior to the hydrogen reduction step. Thus it is possible that under some conditions H_2O may inhibit sintering of Pt catalysts just as it does on planar substrates.

SUMMARY

Sintering rates of Pt on planar SiO_2 surfaces are markedly enhanced by the presence of O_2, while they are inhibited by H_2O, and we suggest that this may be due to the effects of these gases on surface diffusion of Pt on the SiO_2 surface rather than vapor transport of PtO_2.

Particles are crystalline down to diameters of at least 20 Å, although there is a high incidence of single and multiple twins even for small particles. There is no evidence for solid platinum oxide formation upon heating in O_2 in that diffraction showed no oxide crystalline phases and diffraction peak widths indicated crystal sizes comparable to geometric sizes. Gases do not appear to enhance twin formations because there is a comparable incidence of twins in the 500 to 700°C range both in air and in N_2. No evidence of variations of radii of edges or corners of particles was noted in different gas environments.

In a future paper, we will show that a separate oxide phase can be formed upon heating Pt–Pd alloy on SiO_2 in air and that upon decomposition or reduction of the oxide quite different morphologies can be obtained.

REFERENCES

1. Fornwalt, D., and Kinoshita, K., *Micron* **4**, 99 (1973).
2. Bett, J. A., Kinoshita, K., and Stonehart, P., *J. Catal.* **35**, 307 (1974).
3. Flynn, P. C., and Wanke, S. E., *J. Catal.* **33**, 233 (1974).
4. Flynn, P. C., and Wanke, S. E., *J. Catal.* **37**, 432 (1975).
5. Sawruk, S., Rohrman, A. C., Jr., and Kokotailo, G. T., *J. Catal.* **40**, 379 (1976).
6. Kefeli, L. M., *Russ. J. Phys. Chem.* **44**, 1607 (1970).
7. Moss, R. L., *Platinum Metals Rev.* **11**, 141 (1967).
8. Adams, C. R., Benesi, H. A., Curtis, R. M., and Meisenheimer, R. G., *J. Catal.* **1**, 336 (1962).
9. Benesi, H. A., Curtis, R. M., and Studer, H. P., *J. Catal.* **10**, 328 (1968).
10. Wynblatt, P., and Gjostein, N. A., *Scr. Met.* **7**, 969 (1973).
11. Baker, R. T. K., Thomas, C., and Thomas R. B., *J. Catal.* **38**, 510 (1975).
12. Chakraverty, B. K., *J. Phys. Chem. Solids* **28**, 2401 (1967).

13. Flynn, P. C., and Wanke, S. E., *J. Catal.* **34**, 390 (1974).
14. Flynn, P. C., and Wanke, S. E., *J. Catal.* **34**, 400 (1974).
15. Wanke, S. E., *in* "Materials Science Research," Vol. 10: "Sintering and Catalysis" (G. C. Kuczynski, Ed.), p. 107, Plenum, New York, 1975.
16. Wynblatt, P., and Gjostein, N. A., *Progr. Solid State Chem.* **9**, 21 (1975).
17. Wynblatt, P., and Ahn, T. M., *in* "Materials Science Research," Vol. 10: "Sintering and Catalysis" (G. C. Kuczynski, Ed.), p. 83. Plenum, New York, 1975.
18. Wynblatt, P., and Gjostein, N. A., *Acta Met.* **24**, 1165 (1976).
19. Wynblatt, P., and Gjostein, N. A., *Acta Met.* **24**, 1175 (1976).
20. Ruckenstein, E., and Pulvermacher, B., *AIChE J.* **19**, 356 (1973).
21. Ruckenstein, E., and Pulvermacher, B., *J. Catal.* **29**, 224 (1973).
22. Pulvermacher, B., and Ruckenstein, E., *J. Catal.* **35**, 115 (1974).
23. Ruckenstein, E., and Dadyburjar, D. B., *J. Catal.* **48**, 73 (1977).
24. Bassett, G. A., *in* "Condensation and Evaporation of Solids" (E. Rutner, P. Goldfinger, and J. P. Hirth, Eds.), p. 599. Gordon and Breach, New York, 1964.
25. Thomas, J. M., and Walker, P. L., Jr., *J. Chem. Phys.* **41**, 587 (1964).
26. Walker, P. L., Jr., and Thomas, J. M., *Chem. Eng. Progr.* **63**, 139 (1967).
27. Phillips, W. B., Desloge, E. A., and Skofronick, J. G., *J. Appl. Phys.* **39**, 3210 (1968).
28. Maa, J. S., and Lee, J. I., and Hutchinson, T. E., *in* "Proceedings, 34th Annual Meeting, Electron Microscopy Society of America," p. 648, Florida, 1976.
29. Baker, R. T. K., France, J. A., Rouse, L., and Waite, R. J., *J. Catal.* **41**, 22 (1976).
30. Wong, S., Flytzani-Stephanopoulos, M., Chen, M., Hutchinson, T. E., and Schmidt, L. D., *J. Vac. Sci. Technol.* **14**, 452 (1977).
31. Maat, H. J., and Moscou, L., *in* "Proceedings, 3rd International Congress on Catalysis," Vol. II, p. 1277, 1965.
32. Gruber, H. L., *Anal. Chem.* **34**, 1828 (1962).
33. Hughes, T. R., Houston, R. J., and Sieg, R. P., *Ind. Eng. Chem. Process Des. Develop.* **1**, 96 (1962).
34. Herrmann, R. A., Alder, S. F., Goldstein, M. S., and DeBaun, R. M., *J. Phys. Chem.* **65**, 2189 (1961).
35. Somorjai, G. A., *Prog. Anal. Chem.* **1**, 101 (1968).
36. Huang, F. H., and Li, C.-Y., *Scr. Met.* **7**, 1239 (1973).
37. Dorling, T. A., and Moss, R. L., *J. Catal.* **5**, 111 (1966).
38. Dorling, T. A., Lynch, W. J., and Moss, R. L., *J. Catal.* **20**, 190 (1971).
39. Wilson, G. R., and Hall, W. K., *J. Catal.* **24**, 306 (1972).
40. Maa, J. S., Lee, J. I., and Hutchinson, T. E., *in* "Proceedings, 31st Annual Meeting, Electron Microscopy Society of America," New Orleans 1973.
41. Kooi, E., "The Surface Properties of Oxidized Silicon," p. 34. Springer-Verlag, New York, 1967.
42. Solliard, C., Buffat, Ph., and Faes, F., *J. Crystal Growth*, **32**, 123 (1976).
43. Ino, S., *J. Phys. Soc. Japan* **21**, 346 (1966).
44. Ino, S., and Ogawa, S., *J. Phys. Soc. Japan* **22**, 1365 (1967).
45. Ino, S., *J. Phys. Soc. Japan* **27**, 941 (1969).
46. Ogawa, S., and Ino, S., *J. Crystal Growth* **13/14**, 48 (1972).
47. Avery, N. R., and Sanders, J. V., *J. Catal.* **18**, 129 (1970).
48. Sashital, S. R., Cohen, J. B., Burwell, R. L., Jr., and Butt, J. B., *J. Catal.* **50**, 479 (1977).
49. Schlatter, J. C., *in* "Materials Science Research," Vol. 10: "Sintering and Catalysis," (G. C. Kuczynski, Ed.), p. 141, Plenum, New York, 1975.